

A Systematic Mathematical Modeling Approach for the Design and Machining of Concave-Arc Ball-End Milling Cutters with Constant Helical Pitch

Shand-Dad Liaw^{1*} and Wei-Fang Chen²

¹*Department of Mechanical Engineering, De Lin Institute of Technology,
Taipei, Taiwan 236, R.O.C.*

²*Department of Mechanical Engineering, Far East College,
Tainan, Taiwan 744, R.O.C.*

Abstract

As the use of NC techniques to machine the freeform and complex surfaces of dies and molds has increased, the demand for revolving helical cutters with specialized geometries has risen. This paper develops a systematic modeling approach for the design and NC machining of concave-arc ball-end milling cutters with a constant helical pitch. The section profile of groove and grinding wheel in the NC machining of the concave-arc ball-end milling cutters with constant pitch are concluded. The cutting edge is defined with a constant pitch and the grinding wheel is specified in terms of the maximum radius of the cutter. By employing the envelope and inverse envelope theories, the sections of grinding wheel and the radial feed, axis feed, and relative displacement of the grinding wheel during NC machining of the cutter are systematically designed. Based on the maximum sectional radius of the cutter, the principles of inverse envelope theory are then employed to establish the sectional profile of the grinding wheel required to produce the designed cutter using a two-axes NC machine. Models are then presented to continue the radial and axial feeding velocities of the grinding wheel during machining, together with its relative displacement. The proposed models are verified via computer simulation and are found to yield satisfactory results. The models presented in this study are intended to supply a general reference for the automatic design and manufacture of helical cutters with a constant pitch.

Key Words: Envelope, Helical Groove, Constant Pitch, Mathematical Model, Cutting Edge

1. Introduction

NC machining enables the fabrication of components comprising a variety of freeform and complex surfaces. However, forming such surfaces commonly requires the use of revolving cutters with specialized geometries. Of the various cutters in general use, helical cutters are one of the most common, and are employed in a broad range of machining applications throughout industry. The cutting edges and grooves of these revolving

tools are designed not only to perform a milling operation, but also to enhance chip removal. Therefore, to a large extent, the success of the machining operation is dependent on an appropriate design of the cutter's geometrical features.

The literature contains many investigations into the modeling, design and NC machining of revolving helical cutters. In general, these investigations consider three different basic definitions of the helical angle of the cutter: (1) the angle between the helical curve on the revolving surface and the longitudinal curve [1–11], (2) the angle between the helical curve on the re-

*Corresponding author. E-mail: ufsdliaw@ms5.hinet.net

volving surface and the axis of rotation of the cutter [12–20], and (3) a helical cutting edge with a constant pitch [21–24]. Reference [25] develops a surface of the grinding model for ball-end milling cutters, while [26, 27] discuss the geometry, mechanics and dynamics of general milling cutters. Finally, [28–30] focus on the CAD/CAM design and manufacture of helical milling cutters.

In [16], the authors concluded that the first and second definitions of the helical angle were overly complex when applied to develop mathematical descriptions of the cutting edge. It was shown that the cutting edge designed for a cutter with a constant pitch was smoother than that produced by the first two definitions. In [21–23], the authors developed general models for revolving cutters with a constant pitch, but did not specifically address the case of concave-arc ball-end milling cutters. Furthermore, the mathematical models were not verified via computer simulations. Therefore, the objective of the present study is to develop a mathematical model of a concave-arc ball-end milling cutter with constant pitch. Having constructed this model, the study then defines the profile of the grinding wheel required for its manufacture and specifies the feeding speeds and displacements of the grinding wheel during two-axes NC machining of the designed cutter. Finally, the proposed models are verified via computer simulations.

The remainder of this paper is organized as follows. Section 2 develops a mathematical model for the helical groove profile on the cylindrical shank of the cutting tool. Section 3 then constructs a model for the cutting edge on the ball-end part of the cutter and demonstrates how continuity is achieved between this cutting edge and that on the revolving surface of the tool. Section 4 employs inverse envelope theory to design the sectional profile of the grinding wheel required to machine the cutting edge designed in Sections 2 and 3. Section 5 develops models to define the radial and axial feeding speeds of the grinding wheel, and its relative displacement, during two-axes NC machining of the designed cutter. It is also shown how the problem of a residual revolving surface on the ball-end part of the cutter can be overcome by carefully controlling the feed of the grinding wheel in the radial direction. Section 6 verifies the developed models via computer simulations. Finally, Section 7 presents some brief conclusions.

2. Helical Groove Profile on Cylindrical Shank of Cutting Tool

As shown in Figure 1, the helical groove profile on the concave-arc ball-end milling cutter consists of five segments, i.e. three line segments and two arc segments. The first segment (line AB) is tangent to the second segment (arc BC) at point B. Arc BC is tangent to the third segment (arc CD) at point C. Arc CD is tangent to the fourth segment (line DE) at point D. Finally, line DE is tangent to the fifth segment (line EF) at point E. The line segment EF represents the cutting edge zone. The cutting edge on the cylindrical part of the cutter is defined by the continuous spiral motion of the helical groove. In general, the shape of revolving helical cutters is not constant for all machining applications, but varies to meet the requirements of particular machining tasks. Clearly, the depth of the helical groove depends on the radius of the particular cutter. Specifically, as the radius of the cutter decreases, the depth of the groove must be correspondingly reduced. In the present analysis, the sectional design of the cutter groove is based on the maximum outer radius of the cutter.

As discussed above, the helical groove can be defined in terms of five discrete segments. The complete groove section can be described mathematically by using a unit step function to combine the equations describing each of the five segments, i.e.

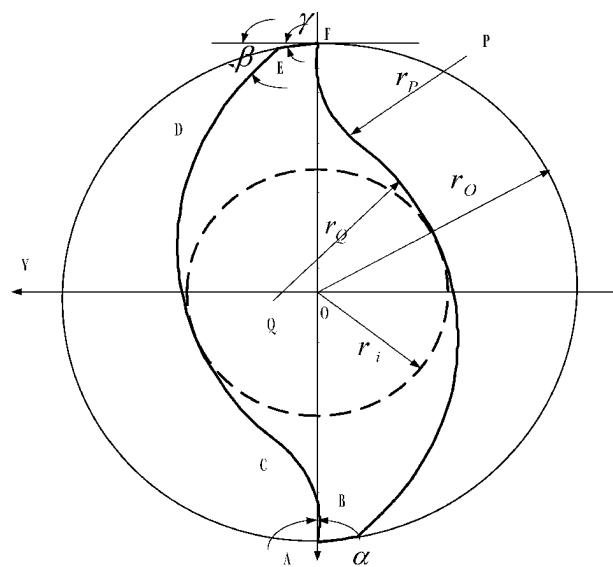


Figure 1. Helical groove profile on concave-arc ball-end milling cutter.

$$\begin{aligned} \mathbf{r} = \{x(t), y(t)\} &= r_{AB}[H(\rho) - H(\rho - 1)] \\ &+ r_{BC}[H(\rho - 1) - H(\rho - 2)] + r_{CD}[H(\rho - 2) - H(\rho - 3)] \\ &+ r_{DE}[H(\rho - 3) - H(\rho - 4)] + r_{KL}[H(\rho - 4) - H(\rho - 5)] \end{aligned} \quad (1)$$

where $H(\rho)$ is a unit step function and ρ is a parameter of the five segments. If the cutter has two helical grooves (as shown in Figure 1), the equations of the five segments are given as:

$$\begin{cases} r_{AB} = \{r_o - AB * \rho * \cos \alpha, -AB * \rho * \sin \alpha\} \\ r_{BC} = \left\{ \begin{aligned} &x_p + r_p \cos[(\rho - 1)(\theta_C - \theta_B) + \theta_B], \\ &y_p + r_p \sin[(\rho - 1)(\theta_C - \theta_B) + \theta_B] \end{aligned} \right\} \\ r_{CD} = \left\{ \begin{aligned} &x_Q + r_Q \cos[(\rho - 2)(\theta_D - \theta_C) + \theta_C], \\ &y_Q + r_Q \sin[(\rho - 2)(\theta_D - \theta_C) + \theta_C] \end{aligned} \right\} \\ r_{DE} = \{x_E + DE*(4 - \rho) \sin \beta, y_E + DE*(\rho - 4) \cos \beta\} \\ r_{EF} = \{x_F + l*(5 - \rho) \sin \gamma, y_F + l*(5 - \rho) \cos \gamma\} \end{cases} \quad (2)$$

where r_o is the maximum radius of the cutter, r_p is the radius of circle P, r_Q is the radius of circle Q, α is the rake angle of the line segment AB with the X-axis, β is the angle of the line segment DE with the Y-axis, γ is the clearance angle of the cutting strip AB with the Y-axis, l is the length of the cutting edge strip EF, θ_B is the angular position of point B on circle P, θ_C is the angular position of point C on circle P, θ_D is the angular position of point D on circle Q, and θ_E is the angular position of point E on circle Q.

The equation of the helical groove on the cylindrical part of the cutter is given by:

$$\begin{aligned} \mathbf{r}_1 &= \{x_1, y_1, z_1\} \\ &= \left\{ \begin{aligned} &x(t) \cos \theta - y(t) \sin \theta, \\ &x(t) \sin \theta + y(t) \cos \theta, \\ &\frac{T\theta}{2\pi} \end{aligned} \right\} \end{aligned} \quad (3)$$

where θ is the revolving angle and T is the thread pitch. A 3-D representation of the helical groove is shown in Figure 2.

3. Continuity of Cutting Edge on Cylindrical Shank and Ball-End Regions of Concave-Arc Milling Cutter

As shown in Figure 3, the profile of a revolving cut-

ter with a concave-arc generator is formed by rotating the curve GHIJ around the Z-axis. The radius of arc GH is R_o and the center angle of arc HI is determined in accordance with the particular machining situation. In other words, the center point S of arc HI may have many different positions relative to the center point O of arc GH. However, this study considers only the case where the straight line OS is perpendicular to the Z-axis. The radius of the concave arc HI is denoted by R_s and the straight line IJ is parallel to the Z-axis. The revolving surface formed by rotating GHIJ around the Z-axis can be expressed by a sectional-continuous function.

The equation of the revolving surface corresponding to arc GH is expressed by:

$$\begin{aligned} \mathbf{r}_{GH} &= \{R_o \cos \delta \cos \theta, R_o \cos \delta \sin \theta, -R_o \sin \delta\} \\ \delta &\in [0, \pi / 2] \quad \theta \in [0, 2\pi] \end{aligned} \quad (4)$$

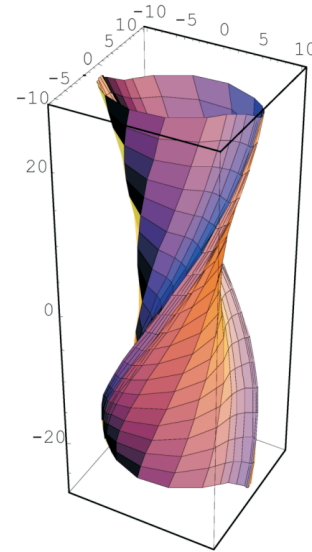


Figure 2. 3-D representation of helical groove.

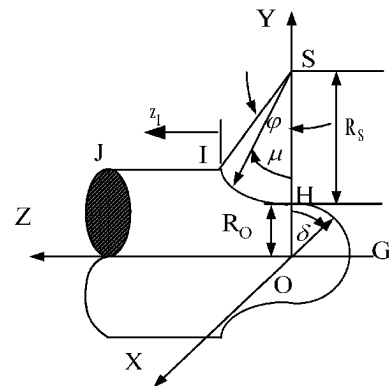


Figure 3. Geometry of concave-arc ball-end milling cutter.

In this study, the cutting edge on this revolving surface is assumed to be a helical curve with a constant thread pitch, T , defined as:

$$T = 2\pi R_o \cos \delta \tan \phi \quad (5)$$

The helical angle ϕ between the cutting edge and the generator of the revolving surface is a function of δ and b , where b is the spiral parameter. Specifically, the helical angle can be defined as:

$$\tan \phi = \frac{T}{2\pi R_o \cos \delta} = \frac{b}{R_o \cos \delta} \quad (6)$$

The partial differential equations of the revolving surface corresponding to arc GH can be expressed as:

$$\frac{\partial \mathbf{r}_{GH}}{\partial \delta} = \mathbf{r}_{GH\delta} = \{-R_o \sin \delta \cos \theta, -R_o \sin \delta \sin \theta, -R_o \cos \delta\} \quad (7)$$

$$\frac{\partial \mathbf{r}_{GH}}{\partial \theta} = \mathbf{r}_{GH\theta} = \{-R_o \cos \delta \sin \theta, R_o \cos \delta \cos \theta, 0\} \quad (8)$$

The coefficients of the first fundamental form are given by:

$$\begin{cases} E = \mathbf{r}_{GH\delta}^2 = (-R_o \sin \delta)^2 + (-R_o \cos \delta)^2 = R_o^2 \\ F = \mathbf{r}_{GH\delta} \cdot \mathbf{r}_{GH\theta} = 0 \\ G = \mathbf{r}_{GH\theta}^2 = (R_o \cos \delta)^2 \end{cases} \quad (9)$$

Defining the helical angle ϕ as the angle between the tangent line $d\mathbf{r}_{GH}$ of the cutting edge and the generator $D\mathbf{r}_{GH}$ ($D\theta = 0$) of the revolving surface, it can be shown that:

$$d\mathbf{r}_{GH} = \mathbf{r}_{GH\delta} d\delta + \mathbf{r}_{GH\theta} d\theta \quad (10)$$

$$D\mathbf{r}_{GH} = \mathbf{r}_{GH\delta} D\delta \quad (11)$$

$$\cos^2 \phi = \frac{(d\mathbf{r}_{GH} \cdot D\mathbf{r}_{GH})^2}{|d\mathbf{r}_{GH}|^2 |D\mathbf{r}_{GH}|^2} \quad (12)$$

Hence, it can be shown that:

$$\frac{d\theta}{d\delta} = \frac{\tan \phi}{\cos \delta} = \frac{b}{R_o \cos^2 \delta} \quad (13)$$

In other words:

$$\theta = \int_0^\delta \frac{b}{R_o \cos^2 \delta} d\delta + \theta_0 = \frac{b}{R_o} \tan \delta + \theta_0 \quad (14)$$

where θ_0 is the initial value of parameter θ . Let the initial $\theta = 0$ when $\delta = 0$, so $\theta_0 = 0$. Therefore, Eq. (14) becomes:

where θ_0 is the initial value of parameter θ . Let the initial $\theta = 0$ when $\delta = \pi/2$, so $\theta_0 = 0$. Therefore, Eq. (14) becomes:

$$\theta = \frac{b}{R_o} \tan \delta \quad (15)$$

The equation of the cutting edge on the revolving surface corresponding to arc GH can be obtained by substituting Eq. (15) into Eq. (4).

As shown in Figure 3, the equation of the revolving surface corresponding to the concave arc HI is given by:

$$\mathbf{r}_{HI} = \{[R_o + R_s(1 - \cos \mu)] \cos \theta, [R_o + R_s(1 - \cos \mu)] \sin \theta, R_s \sin \mu\}, \mu \in [0, \varphi], \theta \in [0, 2\pi] \quad (16)$$

$$\frac{d\theta}{d\mu} = \frac{R_s \tan \phi}{R_o + R_s(1 - \cos \mu)} = \frac{bR_s}{[R_o + R_s(1 - \cos \mu)]^2} \quad (17)$$

Integrating Eq. (17) gives:

$$\theta = bR_s \int_0^\mu \frac{1}{[R_o + R_s(1 - \cos \mu)]^2} d\mu + \theta_1 \quad (18)$$

where θ_1 is the initial value of parameter θ for the revolving surface corresponding to arc HI. At the conjunction position, let the initial $\theta = 0$ when $\mu = 0$, so $\theta_1 = 0$. Therefore, Eq. (18) becomes:

$$\theta = bR_s \int_0^\mu \frac{1}{[R_o + R_s(1 - \cos \mu)]^2} d\mu \quad (19)$$

The equation of the cutting edge for the revolving surface corresponding to arc HI can then be obtained by substituting Eq. (19) into Eq. (16).

As shown in Figure 3, the equation of the revolving surface corresponding to the line segment IJ can be ob-

tained as:

$$\mathbf{r}_{IJ} = \left\{ [R_O + R_S(1 - \cos\phi)]\cos\theta, [R_O + R_S(1 - \cos\phi)]\sin\theta, R_S \sin\phi + z_I \right\} \theta \in [0, 2\pi], z_I \in [0, z_0] \quad (20)$$

$$\frac{d\theta}{dz_I} = \frac{\tan\phi}{R_O + R_S(1 - \cos\phi)} = \frac{b}{[R_O + R_S(1 - \cos\phi)]^2} \quad (21)$$

Integrating Eq. (21) gives:

$$\theta = \frac{bz_I}{[R_O + R_S(1 - \cos\phi)]^2} + \theta_2 \quad (22)$$

where θ_2 is the initial value of parameter θ for the revolving surface corresponding to line segment IJ. At the conjunction position, let $\theta = bR_S \int_0^\phi \frac{1}{[R_O + R_S(1 - \cos\mu)]^2} d\mu$ when $z_I = 0$. Hence, θ_2 is given by:

$$\theta_2 = bR_S \int_0^\phi \frac{1}{[R_O + R_S(1 - \cos\mu)]^2} d\mu \quad (23)$$

Therefore, Eq. (22) becomes:

$$\theta = \frac{bz_I}{[R_O + R_S(1 - \cos\phi)]^2} + bR_S \int_0^\phi \frac{1}{[R_O + R_S(1 - \cos\mu)]^2} d\mu \quad (24)$$

The equation of the cutting edge for the revolving surface corresponding to the line segment IJ can then be obtained by substituting Eq. (24) into Eq. (20).

Note that the derivations above provide expressions for a helical cutting edge in which the thread pitch is constant and the helical angle is specified in terms of the maximum radius of the cutter.

4. Design of Grinding Wheel Sectional Profile

In designing the sectional profile of the grinding wheel required to produce the cutting edge defined above, the coordinate system $\sigma_1 = [O_1; x_1, y_1, z_1]$ is attached to the grinding wheel and the coordinate system $\sigma = [O; x, y, z]$ is attached to the cutter, as shown in Figure 4. It is observed that the X_1 -axis (grinding wheel) lies on the XOY plane and is orientated at an angle of 30° from the X-axis (cutter). Additionally, the centerline axis of the

grinding wheel lies along the Z_1 axis passing through point O_1 . Finally, O_1Z_1 and OZ are straight lines on different planes having a common normal of O_1O . The equation of line O_1Z_1 in the cutter coordinate system σ can be expressed as:

$$\mathbf{r}_{z_1} = \left\{ \frac{\sqrt{3}}{2}a, \frac{a}{2}, 0 \right\} + \zeta \left\{ \frac{\cos\phi}{2}, -\frac{\sqrt{3}\cos\phi}{2}, \sin\phi \right\} \quad (25)$$

where ϕ is the helical angle and a is the distance between the origins O and O_1 of the $\sigma = [O; X, Y, Z]$ and $\sigma_1 = [O_1; X_1, Y_1, Z_1]$ coordinate systems, respectively. Since the profile of the grinding wheel is a revolving surface, the normal vector of any point on the surface passes through its revolving axis, Z_1 . Therefore, in order to satisfy the condition that every point on the helical groove surface of the cutter is a common tangent point of the grinding wheel profile, the normal vector of these cutter surface points must also pass through the centerline axis of the grinding wheel. In other words, line O_1Z_1 can be expressed mathematically as:

$$\mathbf{r}_{z_1} = \mathbf{r}_\phi = \mathbf{r}^* + \lambda \mathbf{r}_t^* \times \mathbf{r}_\theta^* \quad (26)$$

$$= \left\{ x^* + \lambda N_x^*, y^* + \lambda N_y^*, z^* + \lambda N_z^* \right\}$$

By equating the respective components of the left- and right-hand sides of this equation, it can be shown that:

$$\frac{\sqrt{3}}{2}a + \zeta \frac{\cos\phi}{2} = x^* + \lambda N_x^* \quad (27)$$

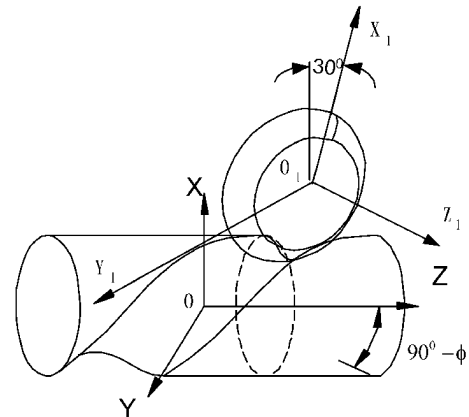


Figure 4. Relative positions of cutter and grinding wheel coordinate systems, σ and σ_1 .

$$\frac{a}{2} - \zeta \frac{\sqrt{3} \cos \phi}{2} = y^* + \lambda N_y^* \quad (28)$$

$$\zeta \sin \phi = z^* + \lambda N_z^* \quad (29)$$

From Eq. (29), it is easily shown that parameter ζ is given by:

$$\zeta = z^* \csc \phi + \lambda N_z^* \csc \phi \quad (30)$$

Substituting Eq. (30) into Eq. (28), it is shown that the parameter λ can be expressed as:

$$\lambda = \frac{a - \sqrt{3} z^* \cot \phi - 2 y^*}{2 N_y^* + \sqrt{3} N_z^* \cot \phi} \quad (31)$$

Substituting Eqs. (30) and (31) into Eq. (27) gives:

$$\begin{aligned} Z^* \cot \phi (N_y^* + \sqrt{3} N_x^*) - N_z^* \cot \phi (\sqrt{3} x^* + y^*) \\ + a(2 N_x^* \cot \phi + \sqrt{3} N_y^* - N_x^*) + 2(y^* N_x^* - x^* N_y^*) = 0 \end{aligned} \quad (32)$$

Exploiting the property of a helical surface, i.e. $y^* N_x^* - x^* N_y^* = b N_z^*$, Eq. (32) can be rewritten as:

$$\begin{aligned} Z^* \cot \phi (N_y^* + \sqrt{3} N_x^*) - N_z^* \cot \phi (\sqrt{3} x^* + y^*) \\ + 2b N_z^* + a(2 N_x^* \cot \phi + \sqrt{3} N_y^* - N_x^*) = 0 \end{aligned} \quad (33)$$

By simultaneously solving Eqs. (3) and (33), the contact curve between the helical groove on the cutter and the profile of the grinding wheel is shown to be:

$$r_j = \{x(\bar{\theta}), y(\bar{\theta}), z(\bar{\theta})\} \quad (34)$$

To obtain the profile of the grinding wheel, the contact curve defined in Eq. (34) must be transformed to the grinding wheel coordinate system, σ_1 . To carry out this transformation, a new coordinate system $\sigma' = [O'; X', Y', Z']$ is introduced. The transformation from coordinate system σ to coordinate system σ' is then given by:

$$\begin{cases} x' = \frac{x}{2} + \frac{\sqrt{3}}{2} y \\ y' = -\frac{\sqrt{3}}{2} x + \frac{y}{2} \\ z' = z \end{cases} \quad (35)$$

Since the origin O_1 and the X_1 - and Z_1 -axes in coordinate system σ_1 are already defined, the direction of the Y_1 -axis can be obtained from the right-hand rule. The transformation from coordinate system σ' to coordinate system σ_1 can then be expressed as:

$$\begin{cases} x_1 = x' - a \\ y_1 = y' \sin \phi + z' \cos \phi \\ z_1 = -y' \cos \phi + z' \sin \phi \end{cases} \quad (36)$$

Hence, the equation of the contact curve can be expressed in terms of the σ_1 coordinate system as:

$$\begin{cases} x_1 = \frac{x(\bar{\theta})}{2} + \frac{\sqrt{3}}{2} y(\bar{\theta}) - a \\ y_1 = \left(-\frac{\sqrt{3}}{2} x(\bar{\theta}) + \frac{y(\bar{\theta})}{2} \right) \sin \phi + z(\bar{\theta}) \cos \phi \\ z_1 = \left(\frac{\sqrt{3}}{2} x(\bar{\theta}) - \frac{y(\bar{\theta})}{2} \right) \cos \phi + z(\bar{\theta}) \sin \phi \end{cases} \quad (37)$$

The profile surface of the grinding wheel can then be computed by rotating the contact curve around the Z_1 -axis. The intersecting curve between the profile surface and the plane $y_1 = 0$ represents the profile curve of the grinding wheel, and can be expressed as:

$$r_c = \left\{ \sqrt{x_1^2 + y_1^2}, 0, z_1 \right\} \quad (38)$$

A grinding wheel with this profile curve will automatically yield the desired groove profile on the cylindrical shank of the helical cutter (designed in Eq. (3)). However, to achieve the designed groove profile on the ball-end portion of the cutter, it is necessary to carefully control the displacement of the grinding wheel in the radial direction, as described below.

5. Continuous Radial and Axial Feeding Speeds of Grinding Wheel during 2-axes NC Machining of Designed Cutter

The revolving surface of a revolving cutter can be expressed by the following general equation:

$$r = \{f(u) \cos \theta, f(u) \sin \theta, g(u)\} \quad (39)$$

The present analysis assumes that the cutter designed in Sections 2 and 3 is to be machined using a two-axis NC machine tool with a grinding wheel rotating at a constant angular velocity, ω . During machining, the feeding speed of the grinding wheel along the axial direction, v_z , is given by:

$$v_z = \frac{dz}{dt} = \frac{dg}{dt} = g' \frac{du}{d\theta} \frac{d\theta}{dt} = \frac{\omega f^2 g'}{b\sqrt{f'^2 + g'^2}} \quad (40)$$

At the revolving surface corresponding to the arc GH of the cutter, the feeding speed of the grinding wheel along the axial direction can be defined as:

$$f = R_o \cos \delta, g = -R_o \sin \delta \quad (41)$$

$$f' = -R_o \sin \delta, g' = -R_o \cos \delta \quad (42)$$

$$v_{z1} = -\frac{\omega R_o^2 \cos^3 \delta}{b} \quad (43)$$

Similarly, at the revolving surface corresponding to the arc HI of the cutter, the feeding speed of the grinding wheel along the axial direction can be defined as:

$$f = R_o + R_s(1 - \cos \mu), g = R_s \sin \mu \quad (44)$$

$$f' = R_s \sin \mu, g' = R_s \cos \mu \quad (45)$$

$$v_{z2} = \frac{\omega [R_o + R_s(1 - \cos \mu)]^2 \cos \mu}{b} \quad (46)$$

At the conjunction point, $\delta = 0$ for the surface given in Eq. (4) and $\mu = 0$ for the surface given in Eq. (16). However, the direction of velocity is reversed compared to $\mu = 0$ for the surface given in Eq. (16) when $\delta = 0$ for the surface given in Eq. (4). Substituting these boundary conditions into Eqs. (43) and (46), respectively, gives:

$$v_{z1} = \frac{\omega R_o^2}{b} = v_{z2} \quad (47)$$

The feeding speed of the grinding wheel in the radial direction must be defined according to a radius function, $f(u)$. If the radial feeding speed varies linearly with the radius, over-cut will occur on the part of the cutter satis-

fying $f(u) < R_o + R_s(1 - \cos \varphi)$. Furthermore, if the radial feeding speed is not appropriately adjusted, the groove will not exist on any part of the cutter at which the radius is less than r_i . Therefore, the appropriate radial feeding displacement must take account both of the general variation $R_o + R_s(1 - \cos \varphi)$ of the cutter radius and the general variation r_i of the feeding displacement. It is assumed that the appropriate feeding displacement, S , varies proportionally with the variation $R_o + R_s(1 - \cos \varphi) - f(u)$ of the cutter radius, i.e.

$$\frac{S}{R_o + R_s(1 - \cos \varphi) - f(u)} = \frac{r_i}{R_o + R_s(1 - \cos \varphi)} \quad (48)$$

Therefore, it can be shown that:

$$\begin{aligned} S &= \frac{[R_o + R_s(1 - \cos \varphi) - f(u)]r_i}{R_o + R_s(1 - \cos \varphi)} \\ &= r_i - \frac{r_i}{R_o + R_s(1 - \cos \varphi)} f(u) \end{aligned} \quad (49)$$

Accordingly, the general equation for the feeding speed of the grinding wheel in the radial direction is given by:

$$\begin{aligned} v_g &= \frac{dS}{dt} = -\frac{r_i}{R_o + R_s(1 - \cos \varphi)} f' \frac{du}{d\theta} \frac{d\theta}{dt} \\ &= -\frac{r_i}{b[R_o + R_s(1 - \cos \varphi)]} \frac{\omega f^2 f'}{\sqrt{f'^2 + g'^2}} \end{aligned} \quad (50)$$

Therefore, when machining the revolving surface corresponding to arc GH of the cutter, the radial speed of the grinding wheel is specified as:

$$v_{g1} = \frac{r_i \omega R_o^2 \cos^2 \delta \sin \delta}{b[R_o + R_s(1 - \cos \varphi)]} \quad (51)$$

$$v_{g1} = \frac{r_i \omega R_o^2 \cos \delta \sin^2 \delta}{b[R_o + R_s(1 - \cos \varphi)]} \quad (51)$$

Similarly, at the revolving surface corresponding to arc HI of the cutter, the radial speed of the grinding wheel is defined as:

$$v_{g2} = \frac{r_i \omega [R_o + R_s(1 - \cos \mu)]^2 \sin \mu}{b[R_o + R_s(1 - \cos \varphi)]} \quad (52)$$

At the conjunction point, $\delta = 0$ for the surface in Eq. (4) and $\mu = 0$ for the surface in Eq. (16). Substituting these boundary conditions into Eqs. (51) and (52), respectively, gives:

$$v_{g1} = 0 = v_{g2} \tag{53}$$

In general, Eqs. (47) and (53) reveal that both the axial and the radial feeding speeds of the grinding wheel vary as continuous functions during two-axis NC machining.

6. Computer Simulation

The design and manufacturing models presented in the sections above for a concave-arc ball-end milling cutter with a constant pitch were verified via computer simulations. The designed cutter was assumed to have the following specification: (1) maximum radius of $r_o = 10$ mm, (2) remaining circular end radius of $r_i = 6$ mm, (3) radius of groove arc BC of $r_p = 4$ mm, (4) radius of groove arc CD of $r_Q = 10$ mm, (5) rake angle of $\alpha = 6^\circ$, (6) clearance angles of cutting strips of $\gamma = 5^\circ$ and $\beta = 45^\circ$, (7) length of cutting edge strip EF of $l = 1$ mm, and (8) cylindrical radius of 10 mm. The sectional profile of the helical groove on the cylindrical shank of the concave-arc ball-end milling cutter is illustrated in Figure 1, while a 3-D representation of the helical groove profile is

shown in Figure 2.

In simulating the results for the grinding wheel profile, the cutter was assigned a thread pitch of $T = 20\sqrt{3}\pi$ mm and a spiral parameter of $b = 10\sqrt{3}$ mm. Furthermore, it was assumed that the distance between the origins of the cutter coordinate system and the grinding wheel coordinate system was 25 mm. Figure 5 presents the results obtained for the sectional profile of the designed grinding wheel, while Figure 6 provides solid rep-

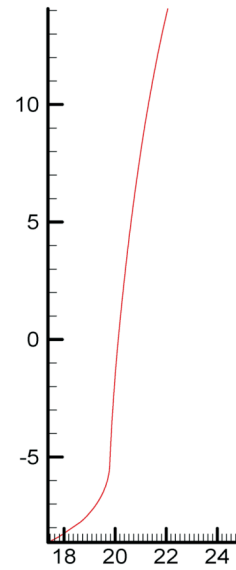


Figure 5. Sectional profile of designed grinding wheel (dimension: mm).

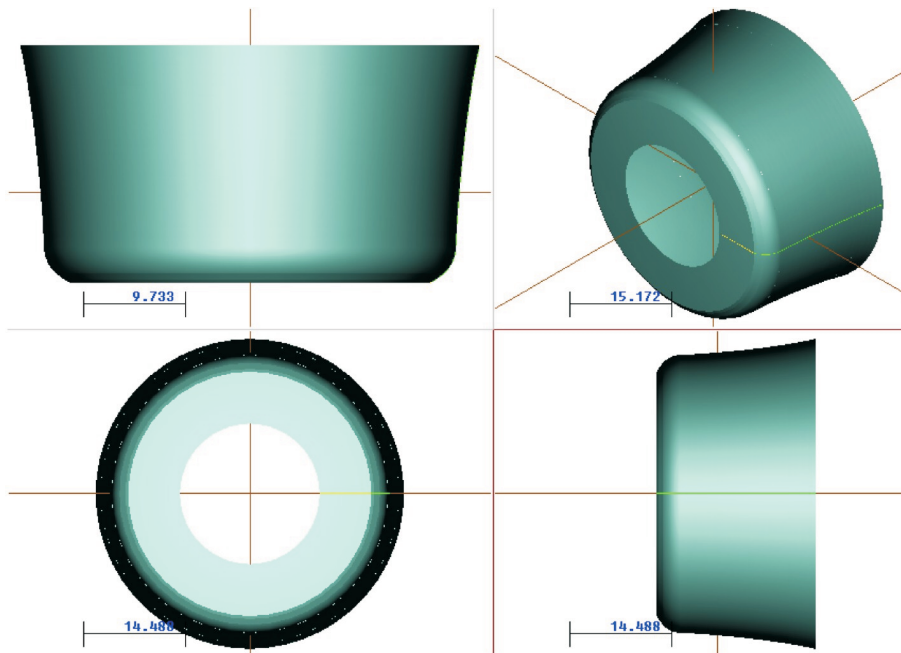


Figure 6. 3-D representations of grinding wheel and sectional profile (dimension: mm).

representations of the grinding wheel and its sectional profile. As shown, a cone-shaped grinding wheel with a rake and bottom angle of $\pi/2 - \gamma$ was used to eliminate the residual surface and to grind the cutting edge strip. The angular velocity of arc HI is $\varphi = \pi/3$ and the speed of the revolving milling cutter is 1 cycle/min. Figure 7 shows the variation in the radius of the revolving surface. As shown, the radius of arc GH on the ball-part of the cutter is $R_o = 5$ mm while the radius of arc HI is $R_s = 10$ mm. Figure 8 shows the variation of the angular parameter for this revolving surface. Figure 9 shows the radial displacement of the grinding wheel. Figure 10 indicates the feeding

speed of the grinding wheel in the axial direction while Figure 11 shows the feeding speed of the grinding wheel in the radial direction. Finally, Figure 12 shows a 3-D schematic of the resulting cutting edge curve with constant pitch formed on the surface of the concave-arc ball-end milling cutter.

7. Conclusion

This paper has presented a systematic mathematical modeling approach for designing and machining the helical groove on a concave-arc ball-end milling cutter with

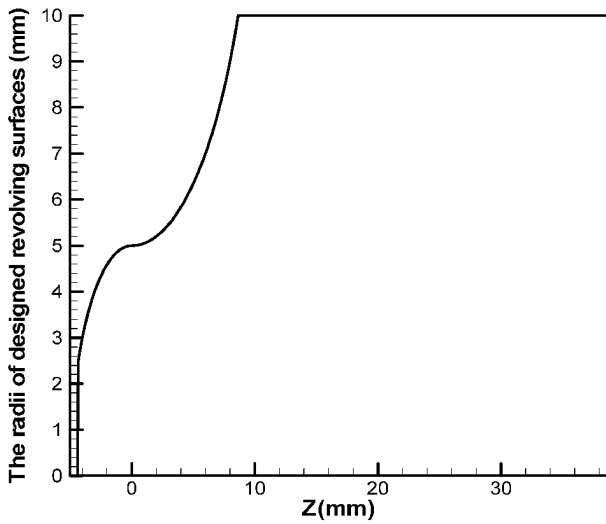


Figure 7. Radii of designed revolving surfaces.

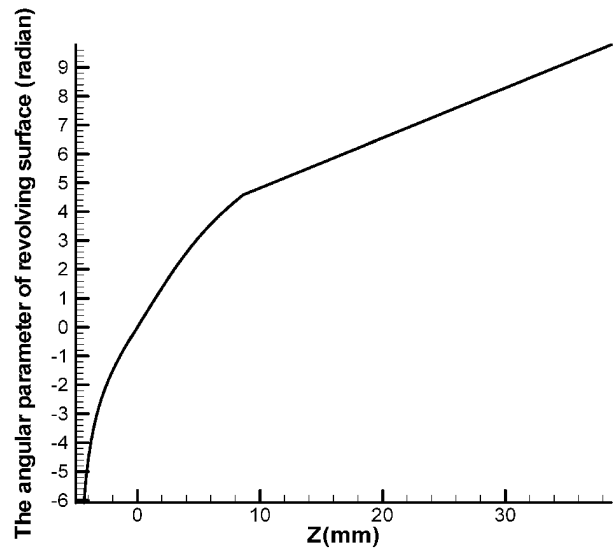


Figure 8. Variation of angular parameter of revolving surface.

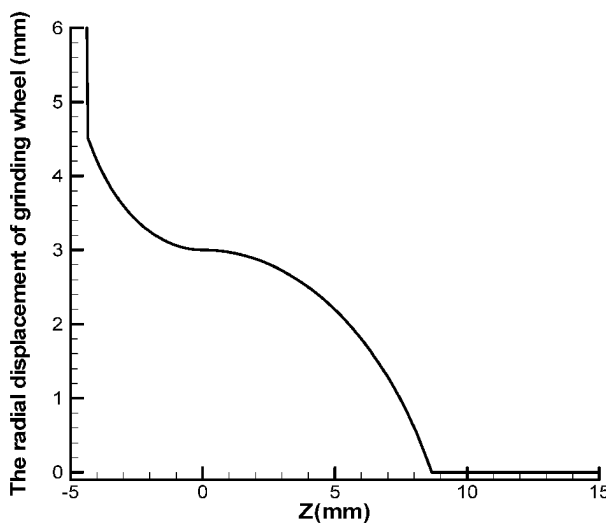


Figure 9. Variation of radial displacement of grinding wheel.

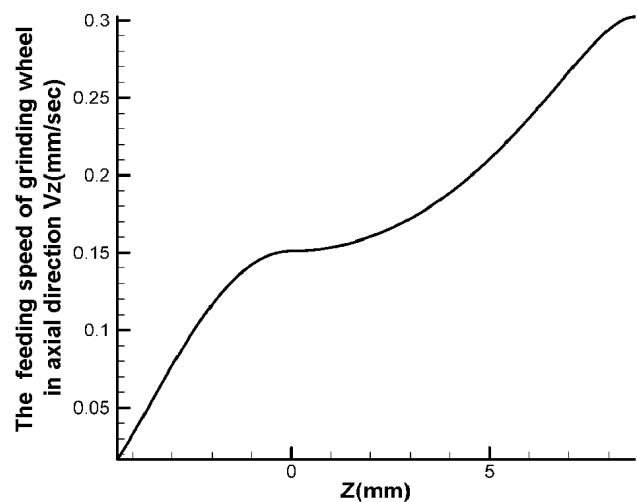


Figure 10. Feeding speed of grinding wheel in axial direction.

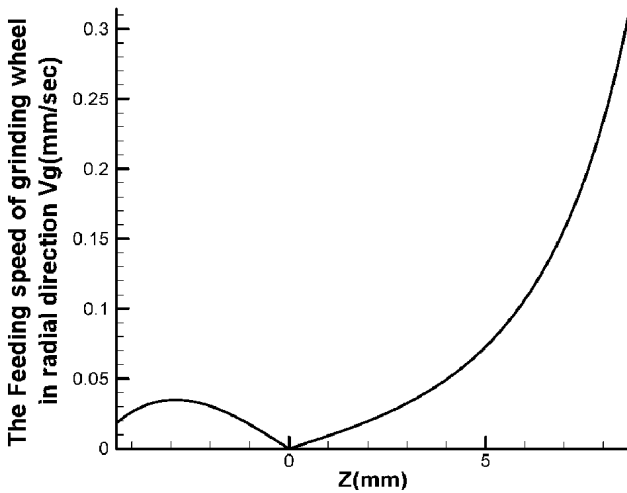


Figure 11. Feeding speed of grinding wheel in radial direction.

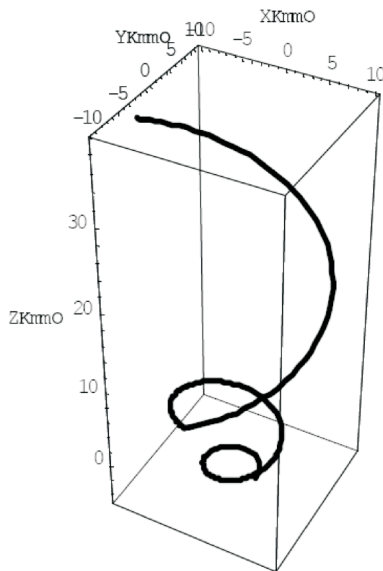


Figure 12. 3-D schematic of helical groove on designed concave-arc ball-end milling cutter.

a constant pitch. The groove surface and the grinding wheel of the enveloping surface should be designed first. According to the maximal sectional radius of the cutter, the profile of the groove section of the grinding wheel is followed by the definition of the profile and relative motion of the grinding wheel. Subsequently, the principles of inverse envelope theory were applied to construct a model for the profile section of the grinding wheel required to generate the designed cutting curve. Finally, expressions for the required axial and radial feeding speeds of the grinding wheel, and its relative displacement during the two-axes NC machining of the designed cut-

ter, were derived. The continuities of the cutting edge and the feeding speed of grinding wheel at the connecting part are verified. The accuracy of the mathematical models was verified via computer simulations. The models of this paper are simulated with an example, and the results are shown to be satisfactory. In conclusion, the modeling method presented in this study provides a valuable approach for the automatic design and machining of concave-arc ball-end milling cutters with two helical grooves of constant pitch.

References

- [1] Wu, C. T. and Chen, C. K., "Study on Rotating Cutters with Different Definitions of Helical Angle," *International Journal of Advanced Manufacturing Technology*, Vol. 17, pp. 627–638 (2001).
- [2] Chen, W. F., Lai, H. Y. and Chen, C. K., "A Precision Tool Model for Concave Cone-End Milling Cutters," *Advanced Manufacturing Technology*, Vol. 18, pp. 567–578 (2001).
- [3] Kaldor, S., Trendler, P. H. H. and Hodgson, T., "Investigation into the Clearance Geometry of End Mills," *Annals of the CIRP*, Vol. 33, pp. 133–139 (1984).
- [4] Kaldor, S., Trendler, P. H. H. and Hodgson, T., "Investigation and Optimization of the Clearance Geometry of End Mills," *Annals of the CIRP*, Vol. 34, pp. 153–159 (1985).
- [5] Kang, S. K., Ehmann, K. F. and Lin, C., "A CAD Approach to Helical Groove Machining Mathematical Model and Model Solution," *Int. J. Mach. Tools Manufact*, Vol. 36, pp. 141–153 (1996).
- [6] Chen, W. F., Lai, H. Y. and Chen, C. K., "Design and NC Machining of Concave-Arc Ball-end Milling Cutters," *Advanced Manufacturing Technology*, Vol. 20, pp. 169–179 (2002).
- [7] Chen, C. K., Lai, H. Y. and Tang, Y., "A Manufacturing Model of Carbide-Tipped Spherical Milling Cutters," *Proc. Inst. Mechanical Engineers. Part B*, Vol. 213, pp. 713–724 (1999).
- [8] Chen, W. F. and Chen, W. Y., "Design and NC Machining of a Toroid-Shaped Revolving Cutter with a Concave Arc Generator," *Journal of Materials Pro-*

- cessing Technology, Vol. 121, pp. 217–225 (2002).
- [9] Kang, S. K., Ehmann, K. F. and Lin, C., “A CAD Approach to Helical Flute Machining Mathematical Model and Model Solution,” *Int. J. Mach. Tools Manufact.*, Vol. 36, pp. 141–153 (1996).
- [10] Wu, C. T., Chen, C. K. and Tang, Y. Y., “Modeling and Computer Simulation of Grinding of the Ball End Type Rotating Cutter with a Constant Helical Angle,” *Proceedings of the Institution of Mechanical Engineers, Part B: Journal of Engineering Manufacture*, Vol. 215, pp. 1–14 (2001).
- [11] Tsai, Y. C. and Hsieh, J. M., “A Study of a Design and NC Manufacturing Model of Ball-End Cutters,” *Journal of Materials Processing Technology*, Vol. 117, pp. 183–192 (2001).
- [12] Chen, W. F., Lai, H. Y. and Chen, C. K., “Design and NC Machining of Concave-Arc Ball-End Milling Cutters,” *Advanced Manufacturing Technology*, Vol. 20, pp. 169–179 (2002).
- [13] Chen, W. Y., Wang, J. C. and Chen, W. F., “A Precision Design and NC Machining of Circular-Arc End-Milling Cutters,” *Journal of Materials Processing & Manufacturing Science*, Vol. 10, pp. 45–67 (2001).
- [14] Chen, W. F., “A Precision Design for Computer Numerical Machining Models of Involute-Generator Revolving Cutters,” *Proceedings of the Institution of Mechanical Engineers Part B-Journal of Engineering Manufacture*, Vol. 218, pp. 517–531 (2004).
- [15] Chen, W. Y., Chang, P. C., Liaw, S. D. and Chen, W. F., “A Study of Design and Manufacturing Models for Circular-Arc Ball-End Milling Cutters,” *Journal of Materials Processing Technology*, Vol. 161(3), pp. 467–477 (2005).
- [16] Chen, W. F., “A Mathematical Solution to the Design and Manufacturing Problems of Ball-End Cutters having a Cutting Edge with Constant Angle to the Axis,” *Journal of Mechanical Engineering Science Proceedings of the Institution of Mechanical Engineers Part C*, Vol. 218, pp. 301–308 (2004).
- [17] Lai, H. Y. and Chen, W. F., “Precision Design and Numerical Control Machining of Tapered Ball-End Milling Cutters,” *Proceedings of the Institution of Mechanical Engineers Part B-Journal of Engineering Manufacture*, Vol. 216, pp. 183–197 (2002).
- [18] Chen, W. Y., Wang, J. C. and Chen, W. F., “A Precision Design and NC Machining of Circular-Arc End-Milling Cutters,” *Journal of Materials Processing & Manufacturing Science*, Vol. 10, pp. 45–67 (2001).
- [19] Lin, S. W., “Study on the 2-Axis NC Machining of a Toroid-Shaped Cutter with a Constant Angle between the Cutting Edge and the Cutter Axis,” *Journal of Materials Processing Technology*, Vol. 115, pp. 338–343 (2001).
- [20] Lin, S. W. and Lai, H. Y., “A Mathematical Model for Manufacturing Ball-End Cutter Using A Two-Axis NC Machine,” *The International Journal of Advanced Manufacturing Technology*, Vol. 17, pp. 881–888 (2001).
- [21] Chen, C. K. and Lin, R. Y., “A Study of Manufacturing Models for Ball-End Type Rotating Cutters with Constant Pitch Helical Grooves,” *International Journal of Advanced Manufacturing Technology*, Vol. 18, pp. 157–167 (2001).
- [22] Ren, B. Y., Tang, Y. Y. and Chen, C. K., “The General Geometrical Models of the Design and 2-Axis NC Machining of a Helical End-Mill with Constant Pitch,” *Journal of Materials Processing Technology*, Vol. 115, pp. 265–270 (2001).
- [23] Wu, C. T. and Chen, C. K., “Manufacturing Models for the Design and NC Grinding of a Revolving Tool with a Circular Arc Generatrix,” *Journal of Materials Processing Technology*, Vol. 116, pp. 114–123 (2001).
- [24] Yan, H. S. and Lin, J. Y., “Geometric Design and Machining of Variable Pitch Lead Screws with Cylindrical Meshing Elements,” *Trans. of the ASME, J. of Mech. Des.*, Vol. 115, pp. 490–495 (1993).
- [25] Lai, H. Y., “A High-Precision Surface Grinding Model for General Ball-End Milling Cutters,” *Advanced Manufacturing Technology*, Vol. 19, pp. 393–402, (2002).
- [26] Engin, S. and Altintas, Y., “Mechanics and Dynamics of General Milling Cutters Part I: Helical End Mills,” *Machine Tools & Manufacture*, Vol. 41, pp. 2195–2212 (2001).
- [27] Engin, S. and Altintas, Y., “Mechanics and Dynamics

- of General Milling Cutters Part II: Inserted Mills,” *Machine Tools & Manufacture*, Vol. 41, pp. 2213–2231 (2001).
- [28] Kaldor, S., Rafael, A. M. and Messinger, D., “On the CAD of Profiles for Cutters and Helical Flutes-Geometrical Aspects,” *Ann. of the CIRP*, Vol. 37, pp. 53–57 (1988).
- [29] Sheth, D. S. and Malkin, S., “CAD/CAM for Geometry and Process Analysis of Helical Groove Machining,” *Annals of the CIRP*, Vol. 39, pp. 129–132 (1990).
- [30] Kang, S. K., Ehmann, K. F. and Lin, C., “A CAD Approach to Helical Groove Machining Mathematical Model and Model Solution,” *Int. J. Mach. Tools Manufacture*, Vol. 36, pp. 141–153 (1996).

Manuscript Received: Jan. 17, 2006

Accepted: Jul. 18, 2006